Flavin Radical Formation in the Light-Oxygen-Voltage-sensing Domain of the Photozipper Blue-light Sensor Protein

[†]Hiroyuki Tsukuno, [†]Kohei Ozeki, [‡]Itsuki Kobayashi, [‡*]Osamu Hisatomi and [†*]Hiroyuki Mino

[†]Division of Material Science, Graduate school of Science, Nagoya University, Chikusa-ku, Furo-cho, Nagoya, 464-8602, Japan, [‡]Department of Earth and Space Science, Graduate School of Science, Osaka University, Osaka, 560-0043, Japan

Supporting Information Placeholder

ABSTRACT: Formation of the neutral flavin radical in the light-oxygen-voltage-sensing (LOV-sensing) domain of photozipper (PZ), based on *Vf*AUREO1, was investigated by electron paramagnetic resonance (EPR) spectroscopy. The flavin radical was observed in the presence of DTT by illumination of a LOV-domain mutant (C254S), in which a photoactive cysteine residue in close proximity to flavin was replaced with a serine. The radical did not form under low initial protein-concentration conditions (less than 20 μM). The flavin radicals accumulated with logistic time-dependent kinetics when the protein concentrations were higher than 30 μM. These results indicate that the radical is produced by concerted reactions involving protein interactions, and that the radical is formed from the LOV dimer but not the LOV monomer. In contrast, logistic time-dependencies were not observed for the sample adapted to the dark following radical formation by illumination, indicating that initialization of the proton pathway is essential for this fast sensing reaction.

1.Introduction

Light-oxygen-voltage-sensing (LOV) domains are widely found in the blue-light (BL) sensor proteins of plants. The LOV domain consists of about 100 amino acids and accommodates a flavin mononucleotide (FMN) as the chromophore. BL induces a conformational change in the LOV domain, which subsequently influences the effector domains, or interactions of other molecules, to induce biological activities. Aureochrome-1 (*Vf*AUREO1) has been proposed to be responsible for the branching response of a stramenopile alga, *Vaucheria frigida*[1, 2]. *Vf*AUREO1 contains an LOV domain and a basic-leucine-zipper (bZIP) domain[3]. The bZIP domain is an α-helical DNA-binding motif found in a family of eukaryotic transcription factors that selectively recognizes sequences in the target DNA[4-8]. AUREO1 was therefore speculated to be a light-regulated transcription factor that binds the target TGACGT DNA sequence[2]. Photozipper (PZ) is an N-terminally truncated AUREO1 consisting of bZIP and LOV domains, and was optimized for cultivation and genetic manipulation[3, 9]. Studies of PZ have clarified that BL induces its dimerization and enhances its affinity for the target DNA sequence[3, 10-15]. Dimerization is a key aureochrome reaction[3, 10-12]; however, the molecular mechanisms that induce the conformational changes of the LOV domains in aureochromes have been poorly clarified to date.

In the first step of the photoreaction of the LOV domain, FMN is excited by BL, which induces the formation of a triplet state. The FMN triplet subsequently induces adduct formation with a highly conserved nearby cysteine residue, which results in a conformational change of the LOV domain. Adduct formation simultaneously transfers a proton from the cysteine to FMN[16-18]. It has been reported that adduct formation is not always required for conversion to the light structure[19, 20]. BL-induced conformational changes were detected even in site-directed mutants whose cysteine residues were substituted with other residues that are unable to form adducts[21-24]. Proton transfer has therefore been speculated to trigger the structural change, namely the conversion of the "dark form" to the "light form" of the LOV domain. Of the photochemical reactions in the blue-light protein, the properties of the flavin radicals have been well characterized by electron paramagnetic resonance (EPR) spectroscopy[25-27].

The crystal structures of LOV domains in aureochromes have been reported[13, 28, 29], but large differences were observed, especially among structures in their light states. Recently, we measured the distance between flavin-radical pairs in the LOV domain of PZ by pulsed electron-electron double resonance (PELDOR)[19]; the measured distance coincides with the FMN-FMN distance in the crystal structure of the LOV dimer in *Phaeodactylum tricornutum Pt*AUREO1a grown under light, suggesting that a similar LOV dimer was formed in solution[13]. Dynamic structural changes in PZ have been observed by time-resolved spectroscopy[30], which revealed that photochemical reactions with timescales of the orders of μs, ms, and sec, are responsible for the formation of dimers composed of light and dark forms.

Herein, we report radical formation in the LOV domain of the cysteine-to-serine mutant (C254S), and propose that initialization of the proton pathway is essential for this fast sensing reaction.

2.Materials and methods

Wild-type expression vectors of PZ and LOV (without the bZIP domain, Fig. S1) were mutated with a PrimeSTAR mutagenesis kit (Takara Bio), using PZ-C254S_F (CGTAACTCCCGCTTCCTGCAAGGTCC) and PZ-C254S_R (GAAGCGGGAGTTACGGCCCAGGATCT) primers, and introduced into BL21(DE3) cells (Invitrogen)[3]. Recombinant PZ and LOV mutants, in which Cys254 was replaced with Ser (C254S), were prepared as described previously[10, 11,19]. Samples were suspended in buffer containing 400 mM NaCl and 20 mM Tris/HCl (pH 7.0). Dithiothreitol (DTT) was added for radical formation such that the final concentration was 1 mM.

X-band (9.64 GHz) Continuous-wave (CW)-EPR experiments were carried using a Bruker ESP-300E EPR spectrometer (Bruker DE) with a dielectric resonator (ER4117DHQH, Bruker DE). Each sample was inserted into a flat quartz cell and illuminated

with a 408 nm diode laser (NDHV220APA, NICHIA; ITC 510, THORLABS) through a 10-mm-diameter glass fiber.

3.Results and Discussion

3.1.Time course for radical formation in the LOV domain

Figure 1A shows the time courses of the EPR signals observed at 20–70 μM LOV-C254S concentrations, acquired at the peak maximum of the flavin radical upon illumination. The trace acquired at 10 μM was used for subtracting unwanted light-induced signals (Figs. S2 and S3). The observed signal was assigned to the flavin neutral radical [19]. The corresponding absorption spectra were shown in Fig. S4. The signal intensities of the flavin neutral radical increased with increasing concentration. It is notable that the flavin signals were induced with a short delay following commencement of illumination. The shapes of these traces are known as "logistic functions". The dotted lines are those fitted according to equation (1):

$$y \propto \frac{y_{max}}{1+(y_{max}/y_0 - 1)e^{-kt}} \qquad (1),$$

where *t*, *y*, and *k* are time, radical concentration, and rate constant, respectively, while y_0 and y_{max} are initial and maximum radical concentrations, respectively. Rate constants *k* (min^{-1}) were estimated to be 0.9–1.0 in the 20–70 μM concentration range, with an average value of 0.98 ± 0.04.

Figure 1B shows the concentration dependence of the EPR signal intensity (y_{max}). It should be noted that radicals did not form at low concentrations, while the signal intensity is linearly proportional to concentration above 30–40 μM. The dotted line is the line of best fit above 40 μM. Using the linear fit, a threshold of about 20 μM was determined for radical formation.

Figure 2 displays time courses of the radical-signal intensities for LOV-C254S (a) in the dark following illumination and (b) re-illuminated following adaptation to the dark. The radical decayed with a time constant of 13 min (trace a). Trace b shows that radicals appeared without any lag time when re-illuminated. No lag time was observed even after long periods in the dark.

Photoexcited flavin molecules form triplet states in reactions of wild-type LOV domains. Both an electron and a proton are subsequently transferred from the nearby cysteine residue (C254), resulting in the formation of an FMN-cysteine adduct. For the C254S mutant, the reaction did not progress after the formation of the triplet state. DTT has two roles: as an electron donor and a proton donor[19]. The flavin radical is produced in the LOV-C254S in the presence of DTT. O_2 molecules in solution have been reported to affect the decay of some mutants in the absence of DTT[20]. However, we confirmed that O_2 degassing in the presence of DTT has no effect in our conditions (Fig. S5). In addition, no concentration dependence of the rate constant *k* (fig. 1) shows that the observed delay time is not caused by parallel reaction with another reactant such as oxygen molecule.

It is remarkable that the time course for radical formation follows a logistic function after initial illumination. Logistic behavior was also observed for the C254A mutant in the presence of DTT (data not shown), and no lag time was observed during the second illumination following adaptation to the dark. Therefore, the C254 mutant appears to initially be in a "resting state" that requires initialization by illumination to become "active".

The overall reaction involves multiple intermediates: the excited state (FMN*) after photon absorption, the triplet state (^{T}FMN) following intersystem crossing, the anion radical ($FMN^{\bullet-}$) after electron transfer; and the neutral radical ($FMNH^{\bullet}$) after proton transfer. During illumination, the FMN molecules become photo-excited with a specific quantum efficiency. FMN* decays so rapidly that the sequence of reactions effectively begins from the ^{T}FMN state.

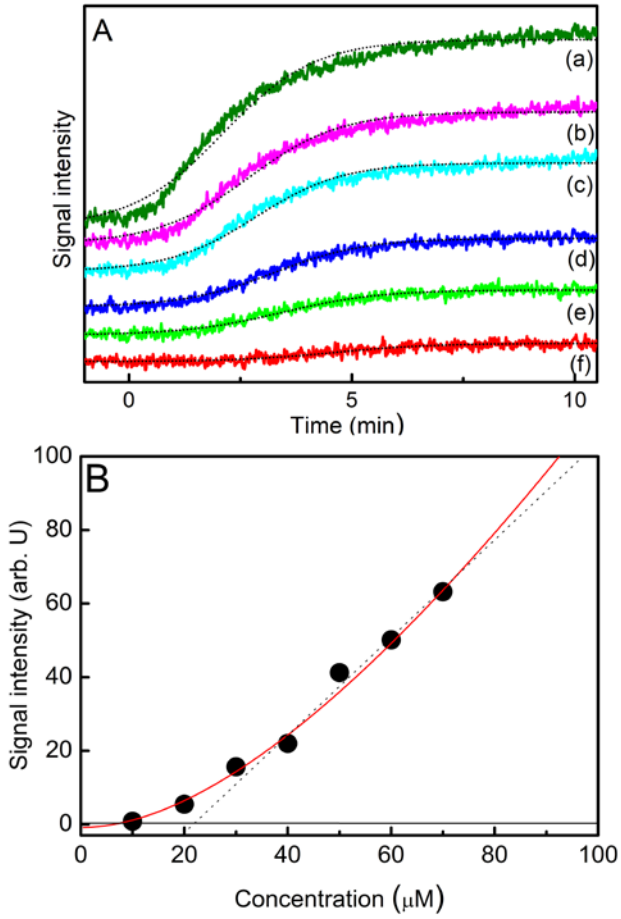

Figure 1. (A) Intensities of the CW-EPR signal of the LOV-C254S as functions of time in the presence of DTT. Illumination commenced at 0 min. The laser power was 30 mW, while the sample concentrations were: (a) 70, (b) 60, (c) 50, (d) 40, (e) 30, and (f) 20 μM. Experimental conditions: microwave frequency, 9.64 GHz; modulation frequency, 100 kHz; modulation amplitude, 15 G; time constant, 655 ms. (B) Maximum signal intensities as a function of sample concentration. The red line was fitted using eq. 3 (K_{total} =370 μM).

$FMNH^{\bullet}$ is generally electrostatically stable because of its lack of charge, but $FMN^{\bullet-}$ is relatively unstable. $FMN^{\bullet-}$ is expected to decay on the order of μs[31], which is significantly faster than subsequent N5 protonation and the conformational change that induces dimerization of the LOV domain. Therefore, the rate-limiting process under illumination is the proton-transfer step leading to $FMNH^{\bullet}$.

3.2.The dependence of radical formation on concentration

The relationship for the formation of the neutral radical in a time-dependent logistic manner, eq. (1), is a solution of the following equation:

$$\frac{dy}{dt} = k(1 - \frac{y}{y_{max}})y \qquad (2),$$

The initial radical concentration $y_{0,}$ is stochastically formed during the initial short time period δt. During y is small, the rate is proportional to the radical concentration y. The rate constant k is the function of the laser intensity. Fig. S6 shows the laser power dependence of the time traces.

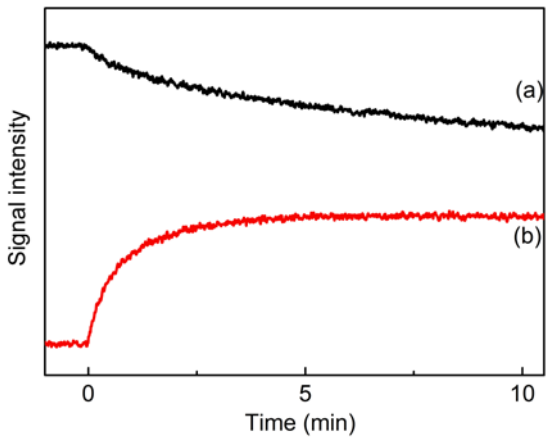

Figure 2: Time courses for (a) radical decay following cessation of illumination and (b) radical formation upon re-illumination. Illumination was terminated at 0 min in (a) and commenced at 0 min in (b). The sample concentration was 70 μM. Experimental conditions are as the same as those reported in Fig 1.

Fig.1 shows that the number of the flavin radicals is approximately proportional to the sample concentration above 40 μM. Such concentration dependence indicates that the radical is produced through a cooperative process with an equilibrium constant of approximately 20–40 μM. The monomers and dimers of wild-type LOV domains have been reported to equilibrate with dissociation constants (K_d) of 30 and 0.6 μM in the dark and light states, respectively[3]. With a K_d value of about 30 μM in the non-radical state, the C254S mutant is assumed to exist in a monomer-dimer equilibrium. Since the decay of $FMN^{\bullet-}$ is faster in the monomeric conformation of the LOV domain than N5 protonation, only a small fraction of the dark form of the LOV domain converted into the light form in the monomeric state. The concentration dependence of radical formation (Fig. 1B) can be explained by the cooperative formation of the neutral radical $FMNH^{\bullet}$ and conversion to the light form as follows. In the dimer state, a dark form of LOV domain paired with the converted light form effectively induces the neutral radical and converts into the light form. The overall reaction is explained by the following model:

$$2[\mathrm{LOV}] \overset{K_d}{\rightleftarrows} [\mathrm{LOV\text{-}LOV}] \overset{K_{inter}}{\rightleftarrows} [\mathrm{LOV\text{-}LOV}]_{inter} \xrightarrow[\text{photon}]{\text{intermediate}} [\mathrm{LOV^{\bullet}\text{-}LOV^{\bullet}}] \qquad \text{rate-limiting}$$

in which [LOV] and [LOV-LOV] represent the molar concentrations of the LOV-domain monomer and dimer in the dark state, respectively. For simplification, the relatively fast decay components, such as [^{T}LOV-LOV], [LOV-^{T}LOV], [^{T}LOV-^{T}LOV], [$LOV^{\bullet-}$-LOV], [LOV-$LOV^{\bullet-}$], and [$LOV^{\bullet-}$-$LOV^{\bullet-}$], are included in $[\mathrm{LOV\text{-}LOV}]_{inter}$. The total equilibrium equation becomes:

$$K_{total} = K_d * K_{inter} = [\mathrm{LOV}]^2 / [\mathrm{LOV^{\bullet}\text{-}LOV^{\bullet}}],$$

where the equilibrium constant K_{inter} includes all of the intermediate states. Based upon a previous calculation[3], the concentration of the neutral radical $LOV^{\bullet}$ can be expressed by the injected sample concentration of the LOV monomer, $[\mathrm{LOV}]_{inj}$, as follows:

$$[\mathrm{LOV^{\bullet}}] = \frac{1}{4}\left\{2 + \frac{K_{inter}K_d}{2[\mathrm{LOV}]_{inj}} - \left\{2 + \sqrt{\left(\frac{K_{inter}K_d}{2[\mathrm{LOV}]_{inj}}\right)^2 + \frac{2K_{inter}K_d}{[\mathrm{LOV}]_{inj}}}\right\}\right\} \times [\mathrm{LOV}]_{inj} \qquad (3).$$

Using eq. (3), the equilibrium constant, K_{total}, which describes the concentration dependence of the radical-signal intensity, was determined to be 370 μM. The concentration dependence of PZ-C254S is almost the same as that of LOV (Fig. S7), although the dissociation K_d of PZ was determined to be 130 μM in the dark[3]. PZ-C254S PZ has two components, the LOV domain and the bZIP domain; consequently, the K_d of PZ does not directly reflect the monomer-dimer equilibrium of its LOV domain at low concentration.

In the wild-type LOV domain, the adduct between flavin and the cysteine residue is immediately formed upon radical formation. The cysteine residue has the dual roles of electron and proton donor. On the other hand, conversion to a light form is not always required to form the adduct[19, 20]. Proton transfer triggers the structural change and possibly involves a Gln (corresponding to Q317 of *Vf*AUREO1). DTT is an electron donor in the C254S mutant. The electron-transfer pathway is determined by the chemical bonds in the protein[32]. The flavin ring is separated by 6–10 Å from the protein surface and the flavin tail is accessible from solution. Therefore, the rate-limiting reaction is not electron transfer, but proton transfer. The electron- and proton-transfer steps are essential for the conversion of the dark form into the light form. As for the recovery reaction, deprotonation of the N5 of flavin in the LOV domain is rate-limiting[33, 34], and adduct formation stabilizes the protonated N5 in the wild type. On the other hand, the radical state is not stabilized prior to N5 protonation in the C254S mutant, where the anion radical probably decays more rapidly than the conformational change of the LOV domain.

3.3.Radical initiation

A lag phase was not detected during radical formation in the sample that had previously produced the radical and was subsequently dark-adapted, indicating that the proton-transfer pathway forms after the formation of the initial neutral radical. Although this process was not detected because of its faster kinetics, a similar proton-transfer mechanism accompanying structural rearrangement would be preserved in the native system.

The main difference between the dark and light structures is the location of the mobile α-helix at the N-terminal of the crystal structure (PDB:5DKK and 5DKL) (Fig. S8). The α-helix in the dark structure might block access from the solvent. Zoltowski et al. classified two sites that regulate the kinetics in the LOV domain: site 1 (FAD, Ile74, Cys76, Thr83, in VVD) and site 2 (Met135, Leu163, Met165 in VVD)[34, 35]. The ability to recruit solvent near N5 was suggested by molecular dynamics simulations[36]. The triangular pocket involving Gln204, Thr101, and N5 (FAD) in ENVOY was similar to that involving Gln350, Val235,

and N5 (FAD) in *Pt*AUREO1a. A tunnel connects Val235 to the surface Thr255-Asn344 residues in *Pt*AUREO1a. If the surface region is covered with the mobile α-helix in the dark structure, the pocket would be inaccessible to water molecules, resulting in a time delay. The interaction with a light form opens the path in the dark form and helps the conversion of the dark form to the light form

3.4. Reaction model under continuous exposure to light

Figure 3 summarizes the overall reaction model. It includes the equilibrium between the monomer and dimer with a dissociation constant, K_d, of 30 μM in the dark state (Fig. 3a). BL-illumination triggers the formation of intermediates without any major structural change between the dark and light forms (from Fig. 3a to 3b). A fraction of the intermediates undergo structural change to the light state (from Fig. 3b to 3c). During association under BL illumination dynamically, fractions of the light form accumulate, where the conversion between the dark and light forms is supported by the dimerization of the light form (Fig. 3c). Finally, the equilibrium of the light form, with a K_d of 0.6 μM, completes the process (Fig. 3d). Continuous exposure to light facilitates the dimerization of the light forms of all molecules. On the other hand, pulse excitation facilitates the dimerization of the light/dark forms of their final products[30].

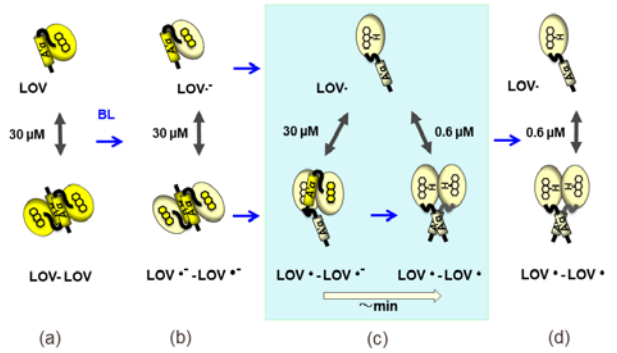

Figure 3. Schematic model for initialization. (a) initial dark state, (b) during initial short illumination, (c) during long illumination and (d) after long illumination. The upper and lower shapes represent monomer and dimer states, respectively. The dark and light forms were represented as folding and stretching shapes. The number of light form is acceleratedly accumulated during the period (c) as chain propagation. See text for details.

In the absence of an external electron and proton donor, such as DTT, no redox event occurs in the LOV-254S domain, even under light. Therefore, the sample conditions around the flavin are preserved immediately after protein purification. The proton-pathway is not constructed in the absence of initialization through pre-illumination. This situation generally occurs in the LOV domain following the usual preparation process under dark condition. The lack of proton-pathway initialization might result in an inactive and/or inhomogeneous structure in the crystal.

AUTHOR INFORMATION

Corresponding Authors
* mino@bio.phys.nagoya-u.ac.jp
* hisatomi@ess.sci.osaka-u.ac.jp

Notes

The authors declare no competing financial interests.

Supporting Information

Schematic drawings of the PZ and LOV domain (Figure S1); time course of CW EPR of the LOV-C254S in the presence of DTT (Figure S2); field-swept EPR spectra of the LOV-C254S in the presence of dithiothreitol (DTT) (Figure S3); absorption spectra of LOV-C254S (Figure S4); time course of CW EPR signals of the untreated and O_2 degassed PZ-C254S in the presence of DTT (Figure S5); Laser power dependence of the time courses for LOVC254S (Figure S6); time course of CW EPR of the PZ-C254S in the presence of DTT (Figure S7); the illustration taken from the crystal structure of aureochrome (Figure S8).

ACKNOWLEDGMENT

This work was partly supported by Nanotechnology Platform Program (Molecule and Material Synthesis) of the Ministry of Education, Culture, Sports, Science and Technology (MEXT), Japan and by a Grant-in-Aid for Scientific Research (C) to O.H. (No. 26440077).

REFERENCES

(1) Takahashi, F., Blue-light-regulated transcription factor, Aureochrome, in photosynthetic stramenopiles. *J. Plant Res.* **2016,** *129*, 189-197.
(2) Takahashi, F., Yamagata, D., Ishikawa, M., Fukamatsu, Y., Ogura, Y., Kasahara, M., Kiyosue, T., Kikuyama, M., Wada, M., and Kataoka, H., AUREOCHROME, a photoreceptor required for photomorphogenesis in stramenopiles. *Proc. Natl. Acad. Sci. U. S. A.* **2007,** *104*, 19625-19630.
(3) Nakatani, Y.; Hisatomi, O., Molecular Mechanism of Photozipper, a Light-Regulated Dimerizing Module Consisting of the bZIP and LOV Domains of Aureochrome-1. *Biochemistry* **2015,** *54*, 3302-3313.
(4) Vinson, C. R.; Sigler, P. B.; McKnight, S. L., Scissors-Grip Model for DNA Recognition by a Family of Leucine Zipper Proteins. *Science* **1989,** *246*, 911-916.
(5) Vinson, C. R.; Hai, T. W.; Boyd, S. M., Dimerization specificity of the Leucine zipper-containing bZIP motif on DNA-binding -prediction and rational design. *Genes Dev.* **1993,** *7*, 1047-1058.
(6) Landschulz, W. H.; Johnson, P. F.; McKnight, S. L., The Leucine Zipper - A Hypothetical Structure Common to a New Class of DNA-Binding Proteins. *Science* **1988,** *240*, 1759-1764.
(7) Fujii, Y.; Shimizu, T.; Toda, T.; Yanagida, M.; Hakoshima, T., Structural basis for the diversity of DNA recognition by bZIP transcription factors. *Nat. Struct. Biol.* **2000,** *7*, 889-893.
(8) Schutze, K.; Harter, K.; Chaban, C., Post-translational regulation of plant bZIP factors. *Trends Plant Sci.* **2008,** *13*, 247-255.

(9) Nakatani, Y.; Hisatomi, O., Quantitative analyses of the equilibria among DNA complexes of a blue-light-regulated bZIP module, Photozipper. *Biophys. Physicobiol.* **2018,** *15*, 8-17.
(10) Hisatomi, O.; Takeuchi, K.; Zikihara, K.; Ookubo, Y.; Nakatani, Y.; Takahashi, F.; Tokutomi, S.; Kataoka, H., Blue light-induced conformational changes in a light-regulated transcription factor, aureochrome-1. *Plant Cell Physiol.* **2013,** *54*, 93-106.
(11) Hisatomi, O.; Nakatani, Y.; Takeuchi, K.; Takahashi, F.; Kataoka, H., Blue light-induced dimerization of monomeric aureochrome-1 enhances its affinity for the target sequence. *J. Biol. Chem.* **2014,** *289*, 17379-17391.
(12) Hisatomi, O.; Furuya, K., A light-regulated bZIP module, photozipper, induces the binding of fused proteins to the target DNA sequence in a blue light-dependent manner. *Photochem. Photobiol. Sci.* **2015,** *14*, 1998-2006.
(13) Heintz, U.; Schlichting, I., Blue light-induced LOV domain dimerization enhances the affinity of Aureochrome 1a for its target DNA sequence. *Elife* **2016,** *5*, e11860.
(14) Herman, E.; Sachse, M.; Kroth, P. G.; Kottke, T., Blue-light-induced unfolding of the Jalpha helix allows for the dimerization of aureochrome-LOV from the diatom Phaeodactylum tricornutum. *Biochemistry* **2013,** *52*, 3094-3101.
(15) Herman, E.; Kottke, T., Allosterically regulated unfolding of the A'alpha helix exposes the dimerization site of the blue-light-sensing aureochrome-LOV domain. *Biochemistry* **2015,** *54*, 1484-1492.
(16) Alexandre, M. T. A.; Domratcheva, T.; Bonetti, C.; van Wilderen, L. J. G. W.; van Grondelle, R.; Groot, M.-L.; Hellingwerf, K. J.; Kennis, J. T. M., Primary Reactions of the LOV2 Domain of Phototropin Studied with Ultrafast Mid-infrared Spectroscopy and Quantum Chemistry. *Biophys. J.* **2009,** *97*, 227-237.
(17) Zoltowski, B. D.; Gardner, K. H., Tripping the Light Fantastic: Blue-Light Photoreceptors as Examples of Environmentally Modulated Protein-Protein Interactions. *Biochemistry* **2011,** *50*, 4-16.
(18) Salomon, M.; Christie, J. M.; Knieb, E.; Lempert, U.; Briggs, W. R., Photochemical and mutational analysis of the FMN-binding domains of the plant blue light receptor, phototropin. *Biochemistry* **2000,** *39*, 9401-9410.
(19) Ozeki, K.; Tsukuno, H.; Nagashima, H.; Hisatomi, O.; Mino, H., Dimeric Structure of the Blue Light Sensor Protein Photozipper in the Active State. *Biochemistry* **2018,** *57*, 494–497.
(20) Yee, E. F.; Diensthuber, R. P.; Vaidya, A. T.; Borbat, P. P.; Engelhard, C.; Freed, J. H.; Bittl, R.; Moglich, A.; Crane, B. R., Signal transduction in light-oxygen-voltage receptors lacking the adduct-forming cysteine residue. *Nat. Commun.* **2015,** *6*, 10079.
(21) Lanzl, K.; von Sanden-Flohe, M.; Kutta, R. J.; Dick, B., Photoreaction of mutated LOV photoreceptor domains from *Chlamydomonas reinhardtii* with aliphatic mercaptans: implications for the mechanism of wild type LOV. *Phys. Chem. Chem. Phys.* **2010,** *12*, 6594-6604.
(22) Lanzl, K.; Noll, G.; Dick, B., LOV1 protein from Chlamydomonas reinhardtii is a template for the photoadduct formation of FMN and methylmercaptane. *ChemBioChem.* **2008,** *9*, 861-864.
(23) Noll, G.; Hauska, G.; Hegemann, P.; Lanzl, K.; Noll, T.; von Sanden-Flohe, M.; Dick, B., Redox properties of LOV domains: Chemical versus photochemical reduction, and influence on the photocycle. *ChemBioChem* **2007,** *8*, 2256-2264.
(24) Guo, H. M.; Kottke, T.; Hegemann, P.; Dick, B., The Phot LOV2 domain and its interaction with LOV1. *Biophys. J.* **2005,** *89*, 402-412.
(25) Kay, C. W., Schleicher, E., Kuppig, A., Hofner, H., Rudiger, W., Schleicher, M., Fischer, M., Bacher, A., Weber, S., and Richter, G., Blue light perception in plants. Detection and characterization of a light-induced neutral flavin radical in a C450A mutant of phototropin. *J. Biol. Chem.* **2003,** *278*, 10973-10982.
(26) Kay, C. W. M.; Elsasser, C.; Bittl, R.; Farrell, S. R.; Thorpe, C., Determination of the distance between the two neutral flavin radicals in augmenter of liver regeneration by pulsed ELDOR. *J. Am.Chem.Soc.* **2006,** *128*, 76-77.
(27) Weber, S.; Mobius, K.; Richter, G.; Kay, C. W. M., The electronic structure of the flavin cofactor in DNA photolyase. *J.Am.Chem.Soc.* **2001,** *123*, 3790-3798.
(28) Banerjee, A.; Herman, E.; Kottke, T.; Essen, L. O., Structure of a Native-like Aureochrome 1a LOV Domain Dimer from Phaeodactylum tricornutum. *Structure* **2016,** *24*, 171-178.
(29) Mitra, D.; Yang, X.; Moffat, K., Crystal structures of Aureochrome1 LOV suggest new design strategies for optogenetics. *Structure* **2012,** *20*, 698-706.
(30) Akiyama, Y.; Nakasone, Y.; Nakatani, Y.; Hisatomi, O.; Terazima, M., Time-Resolved Detection of Light-Induced Dimerization of Monomeric Aureochrome-1 and Change in Affinity for DNA. *J. Phys. Chem. B* **2016,** *120*, 7360-7370.
(31) Kutta, R. J.; Magerl, K.; Kensy, U.; Dick, B., A search for radical intermediates in the photocycle of LOV domains. *Photochem. Photobiol. Sci.* **2015,** *14*, 288-299.
(32) Moser, C. C.; Dutton, P. L., Engineering protein-structure for electron-transfer function in photosynthetic reaction centers. *Biochim. Biophys. Acta* **1992,** *1101*, 171-176.
(33) Pudasaini, A.; Zoltowski, B. D., Zeitlupe Senses Blue-Light Fluence To Mediate Circadian Timing in Arabidopsis thaliana. *Biochemistry* **2013,** *52*, 7150-7158.
(34) Zoltowski, B. D.; Vaccaro, B.; Crane, B. R., Mechanism-based tuning of a LOV domain photoreceptor. *Nat. Chem. Biol.* **2009,** *5*, 827-834.
(35) Zoltowski, B. D.; Schwerdtfeger, C.; Widom, J.; Loros, J. J.; Bilwes, A. M.; Dunlap, J. C.; Crane, B. R., Conformational switching in the fungal light sensor vivid. *Science* **2007,** *316*, 1054-1057.
(36) Lokhandwala, J.; Silverman, Y. d. l. V. R. I.; Hopkins, H. C.; Britton, C. W.; Rodriguez-Iglesias, A.; Bogomolni, R.; Schmoll, M.; Zoltowski, B. D., A Native Threonine Coordinates Ordered Water to Tune Light-Oxygen-Voltage (LOV) Domain Photocycle Kinetics and Osmotic Stress Signaling in Trichoderma reesei ENVOY. *J. Biol. Chem.* **2016,** *291*, 14839-14850.

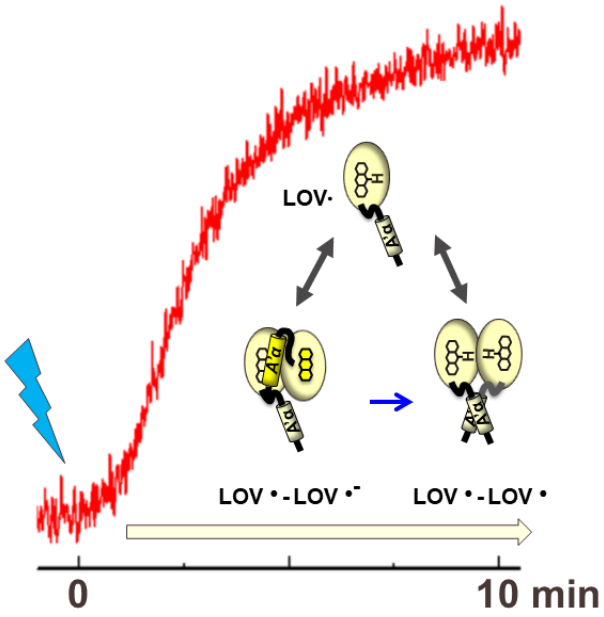

TOC Graphic